



Open
Access

Unsteady Mixed Convection in a Cubic Lid-Driven Cavity Partially Heated from the Bottom

Eutamene Salim¹, Boudebous Saadoun², Berrahil Farid³, Kholai Omar⁴, Dahdi Bachir¹, Filali Abdelkader^{5,*}

¹ Département de Génie Mécanique, Université Mentouri Constantine, Route de Ain El Bey, 25000, Constantine, Algérie

² Département Génie Mécanique, Université Oum El Bouaghi, Algérie

³ Département des Sciences et Techniques, Faculté des Sciences et de la Technologie, Centre Universitaire Abdelhafid Boussouf – Mila, Algérie

⁴ Département de Génie des Transport, Université Mentouri Constantine, Route de Ain El Bey, 25000, Constantine, Algérie

⁵ Département Génie Mécanique, Ecole National Polytechnique de Constantine ENPC, Constantine, Algérie

ARTICLE INFO

Article history:

Received 1 January 2019

Received in revised form 18 April 2019

Accepted 2 May 2019

Available online 17 May 2019

ABSTRACT

A numerical study of transient laminar mixed convection heat transfer characteristics confined within a square (2D) and cubic shape (3D) lid-driven cavity has been carried out. Lateral walls are maintained at a constant cold temperature and move upwards with a constant velocity. A heat source is located at the center of the bottom wall of the cavity and maintained at a constant high temperature. All the remaining parts of the cavity are considered adiabatic. The general conservation equations are discretized according to the Finite Volume method based on the SIMPLER algorithm. Richardson number (Ri) is varied from 0.1 to 10 and the competition between the natural and forced convection forces can lead the flow to adopt, under certain conditions, intricate behaviours such as loss of symmetry, bifurcations and so on. Obtained results showed that the critical Ri numbers that characterize the transition from the forced convection (two symmetric vortices) to the mixed convection (two asymmetric vortices) happens at $Ri = 2.51$ and $Ri = 4.7$ for the 3D and 2d cases, respectively. Then, the second transition from mixed convection to natural convection (four symmetrical vortices) happens at $Ri = 6.29$ and $Ri = 7$ for the 3D and 2d cases, respectively. Results indicated also that the heat transfer process was strongly affected by the dominant heat convection regime in which the rate of heat transfer increased in the case of asymmetric branch which is characterized by a dominance of natural convection mode.

Keywords:

Mixed Convection; Cubic Lid-Driven

Cavity; Finite Volume method;

Richardson number

Copyright © 2019 PENERBIT AKADEMIA BARU - All rights reserved

1. Introduction

Heat transfer in closed cavities is fundamental for various industrial sectors, in particular, those related to energy saving such as cooling of electronic components, building ventilation systems, heat exchangers, solar energy collectors, drying processes, and so on.

* Corresponding author.

E-mail address: filali_abdelkader@yahoo.fr (Filali Abdelkader)

Since Benard's experimental work [1,2] followed by Rayleigh's theoretical work [3], dating back to the early 20th century on natural convection, many experimental, theoretical and numerical studies closely related to Rayleigh-Bénard's convection have been carried out. As is known from the results of most of these studies, the natural convection problem (Rayleigh-Bénard convection) in two or three dimensional confined cavities manifests a strong sensitivity to very feeble deviations in the values of certain parameters such as the Rayleigh (or Grashof) number, the Prandtl number, the aspect ratio of the cavities and the thermal boundary conditions. This phenomenon reveals a variety of complex flow behaviors (instability, symmetry, breaking, bifurcation and chaos) this is highlighted, for example, by the investigations of Gelfgat *et al.*, Erenburg *et al.*, and Lappa [4-7]. Further investigations were highlighted recently by Gelfgat [8].

Mechanism of momentum and energy transport in a two-dimensional geometrical configuration has already been studied extensively in a structured and global way. The dynamic and thermal fields, as well as the effects of relevant parameters specific to this phenomenon, have been determined, analyzed and presented in numerous scientific publications. But until today, this category of research continues to be developed and published in the literature, as evidenced by the work of Hdhiri and Ben Beya, Sivasankaran *et al.*, Ali Khaleel Kareem *et al.*, and Brahim El moustaine and Cheddadi [9-12]. However, all geometric configurations encountered in reality are three-dimensional. Transient three-dimensional natural convection has been the subject to a wide range of very intensive theoretical, experimental, and numerical studies, as witnessed the number of excellent review articles reported in the literature by Yang, Bodenschatz *et al.*, Lappa, Bairy *et al.*, Kadhim Hussein *et al.*, Öztop *et al.*, Soman *et al.*, and Arun *et al.*, [13-20]).

In contrast to time-dependent three-dimensional natural convection, research efforts extended to time-dependent three-dimensional mixed convection have been relatively scarce. So far, only a few studies dealing with this problem have become available in the literature and can mainly be arranged into four categories depending on various combinations of the imposed temperature gradients.

The first category considers cavities heated from below and cooled from the top moving wall. The other remaining walls of the cavity are adiabatic and motionless (the well-known Rayleigh-Bénard convection). Mohammad and Viskanta [21] examine a shallow rectangular cavity filled with liquid gallium, either in the absence or in presence of lid motion. Their experimental and numerical results show that the effect of the lid motion is to reorganize the flow and to make the flow structure quasi-two-dimensional for Richardson numbers less than unity. Prasad and Koseff [22] investigated experimentally the recirculating mixed convection flow within a lid-driven cavity of rectangular cross-section and varying depth, filled with water. Their experimental results present correlations of Nusselt and Stanton numbers obtained from mean values of heat transfer over the entire lower boundary for a wide range of Richardson and Reynolds numbers. Teamah *et al.*, [23] studied numerically the mixed convection in a cubical lid-driven cavity filled with air. Richardson's numbers vary between 0.1 and 10. Among the main results, a correlation has been proposed to link the mean Nusselt number vs the Richardson number at the midsection of the cavity. Abo Elazm *et al.*, [24] considered the same geometric configuration, mentioned earlier, but this time the Richardson number is very small ranging from 5×10^{-5} to 3×10^{-4} . They observed that the average Nusselt number on the upper and lower surfaces decreased for all sections inside the cavity when the Richardson number increases. As in the previous study, a correlation was formulated for each section on both walls for the average Nusselt number as a function of the Richardson number with a maximum error of 7.3%. Ben Mansour *et al.*, [25] have documented another study similar to the two studies already mentioned. They presented the dynamic and thermal field characteristics for Richardson number values ranging from 10^{-3} to 10. In addition, multiple correlations in terms of heat transfer rate and

Richardson number were established. Sidik [26] presented numerical investigation of two-dimensional natural convection in a square cavity heated from bottom and symmetrical cooling from the sides. The study based the lattice Boltzmann method and the well-known finite difference technique is considered. The flow and thermal variables were solved using two different distribution functions. Results indicated that the combination of finite difference with double population thermal lattice Boltzmann model is highly efficient and stable numerical technique for low and moderate Rayleigh number computations. Benderradji *et al.*, [27] conducted numerical simulation of mixed convection problem in three-dimensional cubic cavity subjected to an external flow entering the lower part of the left vertical wall with constant velocity. The investigation focused on the prediction of the flow structure for dominated natural convection (for small values of Re number) and flow structure for dominated forced convection (for high values of Re number). Results showed a Multi clear structure stationary flow regime having cells that strongly depend on Gr and Re numbers. Nusselt number could be expressed a power law function of the form $Nu = c Gr^d$.

The second category examines cavities heated from the top moving wall and cooled from below (stable vertical temperature stratification). It should be noted that in contrast to the first category where the temperature gradient act in parallel to gravity is negative, in this second category, this gradient is always parallel to gravity but positive. Mohammad and Viskanta [28] examined a shallow rectangular cavity filled with water for a range of Rayleigh number and Richardson number. They showed interesting characteristics of the flow behavior, including longitudinal circulations under certain flow conditions. They also concluded that the flow is three or quasi-three dimensional in nature. Iwatsu and Hyun [29] calculated flows in a cubic cavity filled with air. The Reynolds number varies between 10^2 and 2×10^3 whereas the Richardson number varies between 0 and 10. Their results highlight the three-dimensional effects of the flow in the cavity depending on the combination of Reynolds and Richardson numbers. Ouertatani *et al.*, [30] reported a similar numerical study, but in this particular case, the top and the bottom of the cavity move in the same direction with a constant velocity. Numerical simulations were performed by considering Reynolds numbers varying between 10^2 and 10^3 and Richardson numbers varying between 10^{-3} and 10. The authors observed that a remarkable heat transfer improvement of up to 76% could be reached only when the Reynolds number is 400 and the Richardson number is 1.

The third category concerns cavities subject to a temperature gradient imposed via an opposite hot and cold sidewall. Contrary to the well-known Rayleigh–Bénard convection, the temperature gradient, in that case, is perpendicular (Instead of being parallel) to gravity. Benkacem *et al.*, [31] numerically examined a cubic cavity filled with air. Simulations were performed with Reynolds numbers in the range $10^2 \leq Re \leq 10^3$, and Richardson numbers: $10^{-3} \leq Ri \leq 10$. The effects of the different combinations of these numbers on the fluid flow and heat transfer have been presented. More recently, Rani *et al.*, [32] considered exactly the same problem with the same characteristics of the fluid. Sidik and Tanahashi [33] carried out numerical simulation for the natural convection flow in a three-dimensional cubic cavity with hot temperature on the left side and cold temperature on the right side and the other faces were considered adiabatic. The numerical computations were carried out for Rayleigh number of 10^3 , 10^4 and 10^5 to test the validity of the 3D eight-velocity and 3DQ8 thermal lattice Boltzmann model. Results showed a good prediction predicted of the flow features for different Rayleigh numbers.

The fourth category concerns an extension of the old studies of Guo and Sharif [34], and Aydin and Yang [35] from the laminar flow regime in a square cavity to the turbulent flow regime in a cubic square cavity. The sidewalls of the cavity are isothermal and moving in the same direction to gravity, a heat source is placed in the center of the bottom wall. The rest domain parts are adiabatic. Guo and Sharif [34] imposed a constant heat flux whereas Aydin and Yang [35] considered a fixed

temperature. Despite the importance of this geometric configuration (e.g. air cooling of the electronic devices), only very limited works have been published recently by Khaleel Kareem and his co-authors [36-38]. In the previous papers, the commercial CFD code ANSYS®FLUENT is used to solve the governing equations for the turbulent flow regime (The Reynolds number is between 5×10^3 and 3×10^4 whilst the Richardson number is between 1 and 10). Different models such as Reynolds-averaged Navier–Stokes (RANS), unsteady RANS (URANS), and large eddy simulation (LES) were used for turbulence modeling. In Khaleel Kareem and Gao and Khaleel Kareem *et al.*, the cavity is filled with air while in Khaleel Kareem and Gao the cavity is filled with different types of nanofluids with different diameters of nanoparticles [36-38]. They observed interesting behaviors of the thermal and flow fields with changing the Reynolds or Richardson numbers. Increasing these numbers leads to an increase in the number of Nusselt and fluctuations in the kinetic energy of the fluid in the field. In addition, the comparison between the different turbulent models has elucidated clearly the advantages of the LES approach in predicting more detailed heat and flow structures.

In light of these works, it seems interesting to note that buoyancy forces due to temperature gradient and forced convection due to shear forces cooperate to enforce a flow composed of two strictly symmetrical contra-rotating cells about the vertical midline of the moving sidewalls. The case where these two forces act competitively in a laminar flow regime (i.e. the velocity of moving sidewalls is opposite to gravity) has never been considered. This competition between the two forces can lead the flow to adopt, under certain conditions, intricate behaviors such as loss of symmetry, bifurcations and so on. Therefore, we wish to extend the study of Aydin and Yang [35] in a cubic cavity by considering, in this case, the direction of the velocity of the lateral walls constant and opposite to the gravity.

2. Physical Model

The schematic view of the geometric configuration investigated in the present study is shown in Figure 1. It consists of a cubic cavity of side length L . The lateral walls of this cavity are maintained at a constant cold temperature T_c and move upwards with a constant velocity V_0 . A heat source of size $l = 3/5$ of L is located at the center of the bottom wall of the cavity and maintained at a constant high temperature T_h . All remaining parts of the cavity are considered adiabatic.

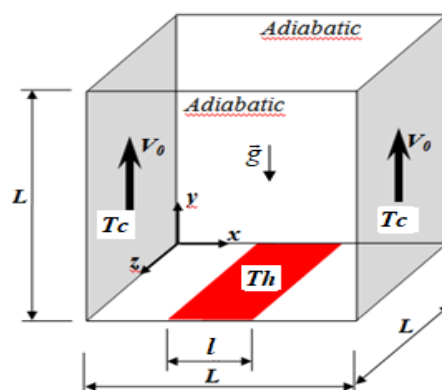


Fig. 1. A schematic diagram of the cubic cavity

3. Mathematical Formulation

The equations that express the conservation of mass, momentum and energy have been written in accordance with the following hypotheses: The flow is considered unsteady, laminar, and incompressible. The viscous dissipation term in the energy equation is neglected. Fluid properties are supposed constant, except the density in the buoyancy term of the momentum equation in the vertical direction (The Oberbeck-Boussinesq approximation). So, governing equations can be expressed in the dimensionless form, in the Cartesian coordinates, as follows

Continuity equation

$$\frac{\partial U}{\partial X} + \frac{\partial V}{\partial Y} + \frac{\partial W}{\partial Z} = 0 \quad (1)$$

Momentum equation

$$\frac{\partial U}{\partial t} + U \frac{\partial U}{\partial X} + V \frac{\partial U}{\partial Y} + W \frac{\partial U}{\partial Z} = -\frac{\partial P}{\partial X} + \frac{1}{\text{Re}} \left(\frac{\partial^2 U}{\partial X^2} + \frac{\partial^2 U}{\partial Y^2} + \frac{\partial^2 U}{\partial Z^2} \right) \quad (2)$$

$$\frac{\partial V}{\partial t} + U \frac{\partial V}{\partial X} + V \frac{\partial V}{\partial Y} + W \frac{\partial V}{\partial Z} = -\frac{\partial P}{\partial Y} + \frac{1}{\text{Re}} \left(\frac{\partial^2 V}{\partial X^2} + \frac{\partial^2 V}{\partial Y^2} + \frac{\partial^2 V}{\partial Z^2} \right) + \text{Ri} \frac{\partial \theta}{\partial Y} \quad (3)$$

$$\frac{\partial W}{\partial t} + U \frac{\partial W}{\partial X} + V \frac{\partial W}{\partial Y} + W \frac{\partial W}{\partial Z} = -\frac{\partial P}{\partial Z} + \frac{1}{\text{Re}} \left(\frac{\partial^2 W}{\partial X^2} + \frac{\partial^2 W}{\partial Y^2} + \frac{\partial^2 W}{\partial Z^2} \right) \quad (4)$$

Energy equation

$$\frac{\partial \theta}{\partial t} + U \frac{\partial \theta}{\partial X} + V \frac{\partial \theta}{\partial Y} + W \frac{\partial \theta}{\partial Z} = \frac{1}{\text{Re} \cdot \text{Pr}} \left(\frac{\partial^2 \theta}{\partial X^2} + \frac{\partial^2 \theta}{\partial Y^2} + \frac{\partial^2 \theta}{\partial Z^2} \right) \quad (5)$$

Here $\text{Re} = V_0 L / \nu$, $\text{Pr} = \nu / \alpha$, $\text{Ri} = \text{Gr} / \text{Re}^2$ and $\text{Gr} = g \beta \Delta T L^3 / \nu^2$ are the Reynolds, the Prandtl, the Richardson and the Grashof numbers, respectively, and $\Delta T = T_h - T_c$ is the temperature difference. The dimensionless variables used for this investigation are:

$$X, Y, Z = \frac{x, y, z}{L}; \quad U, V, W = \frac{u, v, w}{V_0}; \quad \tau = \frac{V_0}{L} t; \quad \theta = \frac{T - T_c}{\Delta T}; \quad P = \frac{p}{\rho V_0^2} \quad (6)$$

The numerical resolution of the previous equations is based on the following initial and boundary conditions

- The initial conditions ($\tau = 0$) are

For the right and left wall

$$V=1 \quad (7a)$$

For the bottom wall

$$\left. \begin{array}{l} Y = 0 \\ 0 \leq Z \leq 1 \\ (1-\varepsilon)/2 \leq X \leq (1+)/2 \end{array} \right\} \Rightarrow \theta = 1. \quad (7b)$$

A zero value is assigned to all variables everywhere else.

- The boundary conditions ($\tau > 0$) are

For the right and left wall

$$\left. \begin{array}{l} X = 0 \\ X = 1 \end{array} \right\} 0 \leq Y \leq 1 \ \& \ 0 \leq Z \leq 1 \Rightarrow U = W = \theta = 0; \quad V = 1. \quad (7c)$$

For the top wall

$$Y = 1 \quad 0 \leq Z \leq 1 \ \& \ 0 \leq X \leq 1 \Rightarrow U = V = W = 0; \quad \frac{\partial \theta}{\partial Y} = 0 \quad (7d)$$

For the bottom wall

$$Y = 0 \ \& \ 0 \leq Z \leq 1 \left\{ \begin{array}{ll} 0 \leq X \leq (1-\varepsilon)/2 & \Rightarrow U = V = W = 0; \quad \frac{\partial \theta}{\partial Y} = 0 \\ (1-\varepsilon)/2 \leq X \leq (1+)/2 & \Rightarrow U = V = W = 0; \quad \theta = 1. \\ (1+\varepsilon)/2 \leq X \leq 1 & \Rightarrow U = V = W = 0; \quad \frac{\partial \theta}{\partial Y} = 0 \end{array} \right. \quad (7e)$$

For the front and back wall

$$\left. \begin{array}{l} Z = 0 \\ Z = 1 \end{array} \right\} 0 \leq X \leq 1 \ \& \ 0 < Y < 1 \Rightarrow U = W = V = 0; \quad \frac{\partial \theta}{\partial Z} = 0. \quad (7f)$$

where $\varepsilon=l/L$ is the dimensionless length of the heat source.

The heat transfer rate at the hot part located at the bottom of the cavity is defined by the local Nusselt number, which is obtained from

$$Nu(x, z) = - \left. \frac{\partial \theta}{\partial Y} \right|_{Y=0} \quad (8)$$

The integral of this number makes it possible to obtain the average Nusselt number.

$$\overline{Nu} = \int_0^1 \left[\int_{(1-\varepsilon)/2}^{(1+\varepsilon)/2} Nu(x, z) dX \right] dZ \quad (9)$$

4. Numerical Procedure

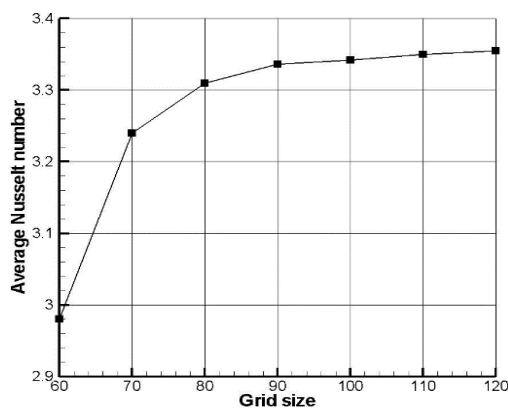
The above set of governing equations, Eq. (1)-(5) subject to the given boundary conditions, Eq. (7a)-(7f) was discretized by a finite volume method using staggered grid. The power law scheme is used in the discretizing procedure to treat the convection and diffusion terms. The pressure-velocity coupling was dealt with SIMPLER algorithm Patankar [39]. The resulting nonlinear algebraic equations are solved using the line-by-line technique, combining the Thomas algorithm (tridiagonal matrix algorithm: TDMA) and the Gauss-Seidel method. The convergence criterion for each variable was examined at each time step. The relative variations of these variables between two successive iterations become smaller than 10^{-6} . The numerical method described above was written using an in-house FORTRAN program.

Grid independence tests is carried out and the calculated average Nusselt number with $Ri = 0.1$, $Re = 100$ and $Pr = 0.71$ are obtained using grid sizes ranging from $61 \times 61 \times 61$ to $121 \times 121 \times 121$, with a spatial increment of 10, as given in Table 1 and presented in Figure 2(a). As a compromise between accuracy and CPU time, a non-uniform grid with $91 \times 91 \times 91$ grid points, as depicted in Figure 2(b), is adopted since the relative error on the average Nusselt numbers is less than 0.6% compared to that of the grid with $121 \times 121 \times 121$ grid points.

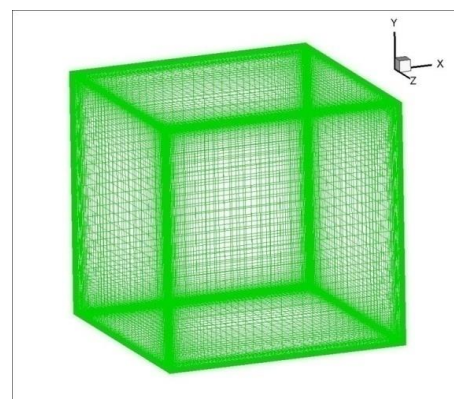
To validate the in-house computational code, a comparison is made with the results of Iwatsu and Hyun [29] with respect to the investigation of mixed convection in a lid-driven cubic cavity with a vertical temperature gradient. The top wall is maintained at a higher temperature than the bottom wall while all the other walls are thermally insulated. The average Nusselt number, for different values of Richardson and Reynolds numbers, indicated in Table 2, shows a very good agreement between the present results and the results obtained by Iwatsu and Hyun [29].

Table 1
 Comparison of average Nusselt Number at different grid sizes

Grid size	Average Nusselt number	Relative Error (%)
$61 \times 61 \times 61$	2.98	11.2
$71 \times 71 \times 71$	3.24	3.45
$81 \times 81 \times 81$	3.31	1.35
$91 \times 91 \times 91$	3.336	0.56
$101 \times 101 \times 101$	3.342	0.39
$111 \times 111 \times 111$	3.35	0.15
$121 \times 121 \times 121$	3.355	-



(a)



(b)

Fig. 2. (a) The effect of grid refinement on the average Nusselt number (b) Schematic view of the grid distribution of computational domain

Table 2

Comparison of the average Nusselt number obtained in the present study with those obtained by Iwatsu and Hyun [29]

		$Re = 10^2$	$Re = 4.10^2$	$Re = 10^3$
Ri = 0.001	Present study	1.825	3.975	6.98
	Iwatsu & Hyun [26]	1.82	3.99	7.03
	Relative Error (%)	0.27	0.37	0.71
Ri = 1	Present study	1.343	1.521	1.789
	Iwatsu & Hyun [26]	1.33	1.50	1.80
	Relative Error (%)	0.97	1.3	0.6
Ri = 10	Present study	1.092	1.158	1.395
	Iwatsu & Hyun [26]	1.08	1.17	1.37
	Relative Error (%)	1.09	1.02	1.79

5. Results and Discussion

Computations are carried out for a fixed Reynolds number $Re=100$ and Prandtl number $Pr = 0.71$. The non-dimensional heated part is kept to 0.6. Results are sketched by gradually increasing Richardson number and compared with 2-D cases. Figure 3 shows the stream lines and isotherms contours at the planes $z = 0.25, 0.5$ and 0.75 for 3D and 2-D cases for Richardson number 0.1, which corresponds to forced convection regime. The flow solution is characterized by a two-symmetric counter rotating cells. The air is essentially driven by the sidewalls shear forces. Due to the subsidiary effect of the buoyant forces, the temperature is stratified at the lower part of the cavity. The air driven to the core of the cavity has lower temperature than the side parts at the same depth. By increasing Richardson number, the buoyant effect becomes more discernible.

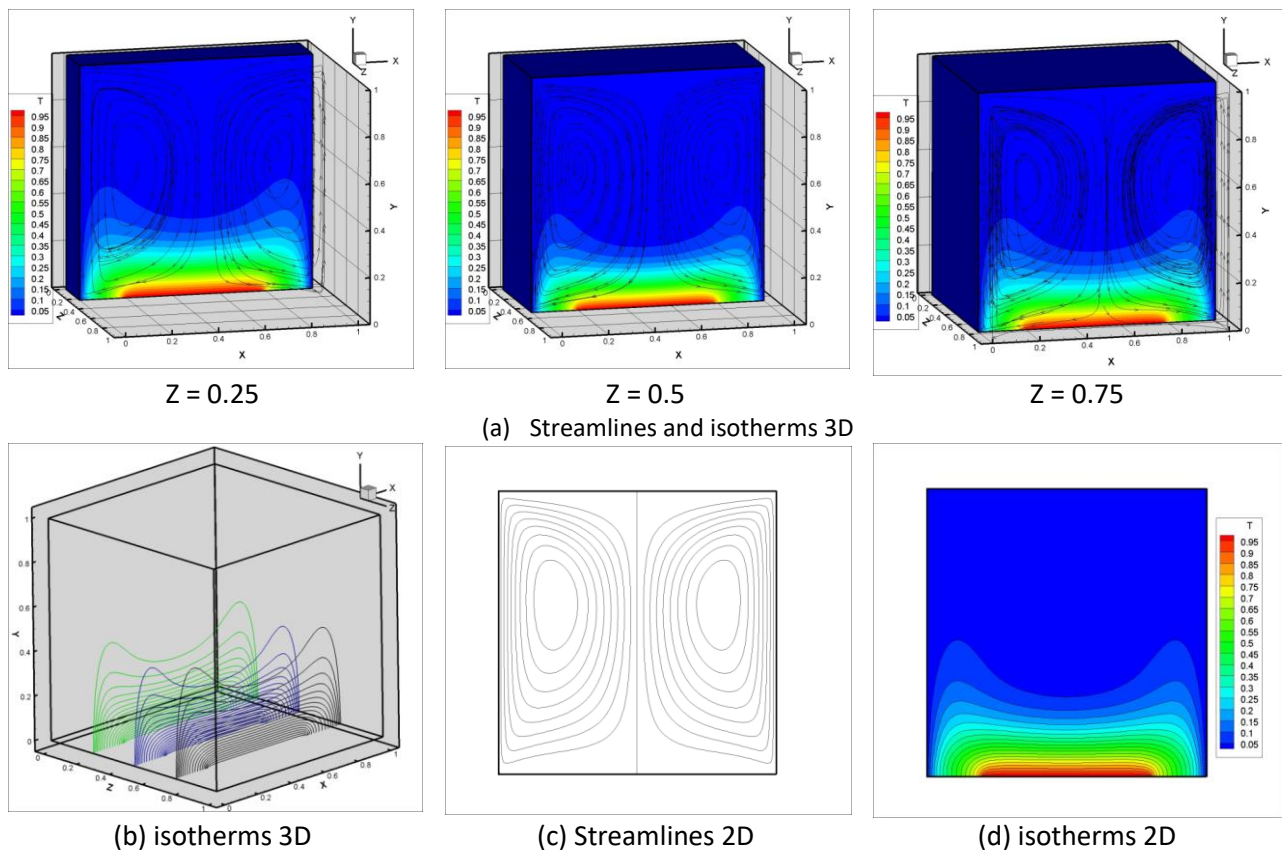


Fig. 3. Streamlines and isotherms for $Re = 100$, Prandtl $Pr = 0.71$ and Richardson number 0.1, (a,b) 3D case, (c,d) 2D case

As Richardson number exceed approximately 2.5 for 3-D case and 4.5 for 2-D case a new branch of solution could be observed, where the solution starts to deviate from the symmetrical behaviour. The onset of deviation starts for a Richardson number between 2.5 and 3 for 3-D case and 4.5 and 5 for 2-D case. Figure 4 represents the plot of stream function and isotherms for $Ri=5$ at the planes $z = 0.25, 0.5, 0.75$ for 3D and 2-D cases. The flow is characterized by an asymmetric counter rotating cells. A large cell occupied the two third of the cavity and a small one on the right side of the cavity. The isotherms show an asymmetric distribution of the temperature as well and the thermal gradient is more pronounced on the left side of the cavity. it was observed that the large cell is a buoyant induced cell and the right one is shear induced one. Note that the current behaviour was not observed in the cases studied by Aydin and Yang [35] and Guo and Sharif [34].

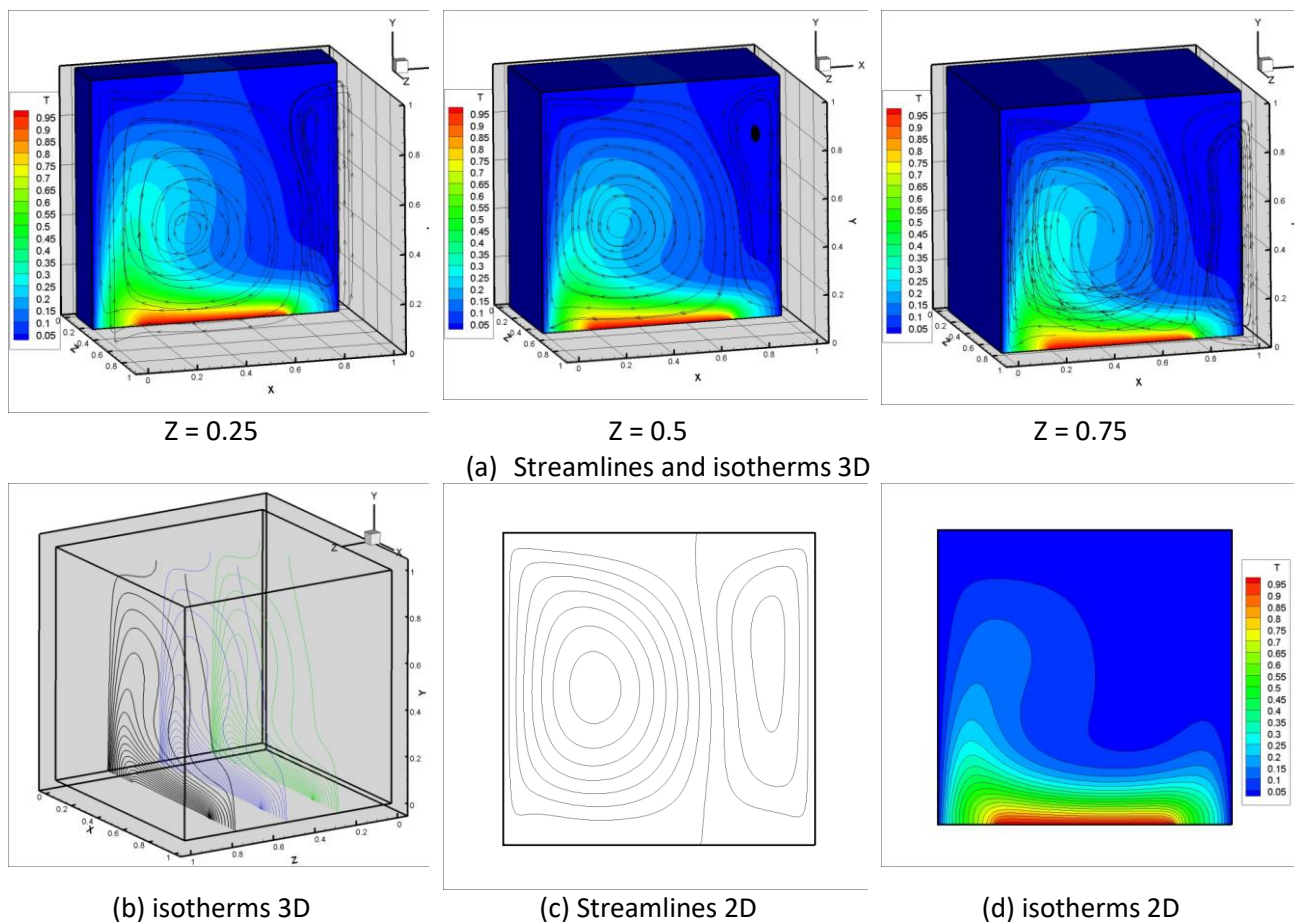


Fig. 4. Streamlines and isotherms for $Re = 100$, Prandtl $Pr = 0.71$ and Richardson number 5, (a,b) 3D case, (c,d) 2D case

An abrupt transition to a new branch solution could be observed as Ri reaches 6.3 (Figure 5). Two pairs of symmetric counter rotating cells characterized the new flow behaviour. Two primary cells at the center of the cavity with a pronounced circulation and the outer cells are stretched near the sidewalls. The results of this investigation discern that the heat transfer rate depend to the nature of convection and the heat source emplacement (high rate near the back and front walls due to the high temperature gradient and minimum at the center of the cavity).

Figure 6 show the temperature isosurfaces distribution at the cavity from $\theta = 0.9$ at the bottom to $\theta = 0.1$ at the top, in the three cases studied the back half domain in $(0 < z < 0.5)$ is symmetric to the front half $(0.5 < z < 1)$ and the part affected by heat transfer near the walls is high than the center of the cavity.

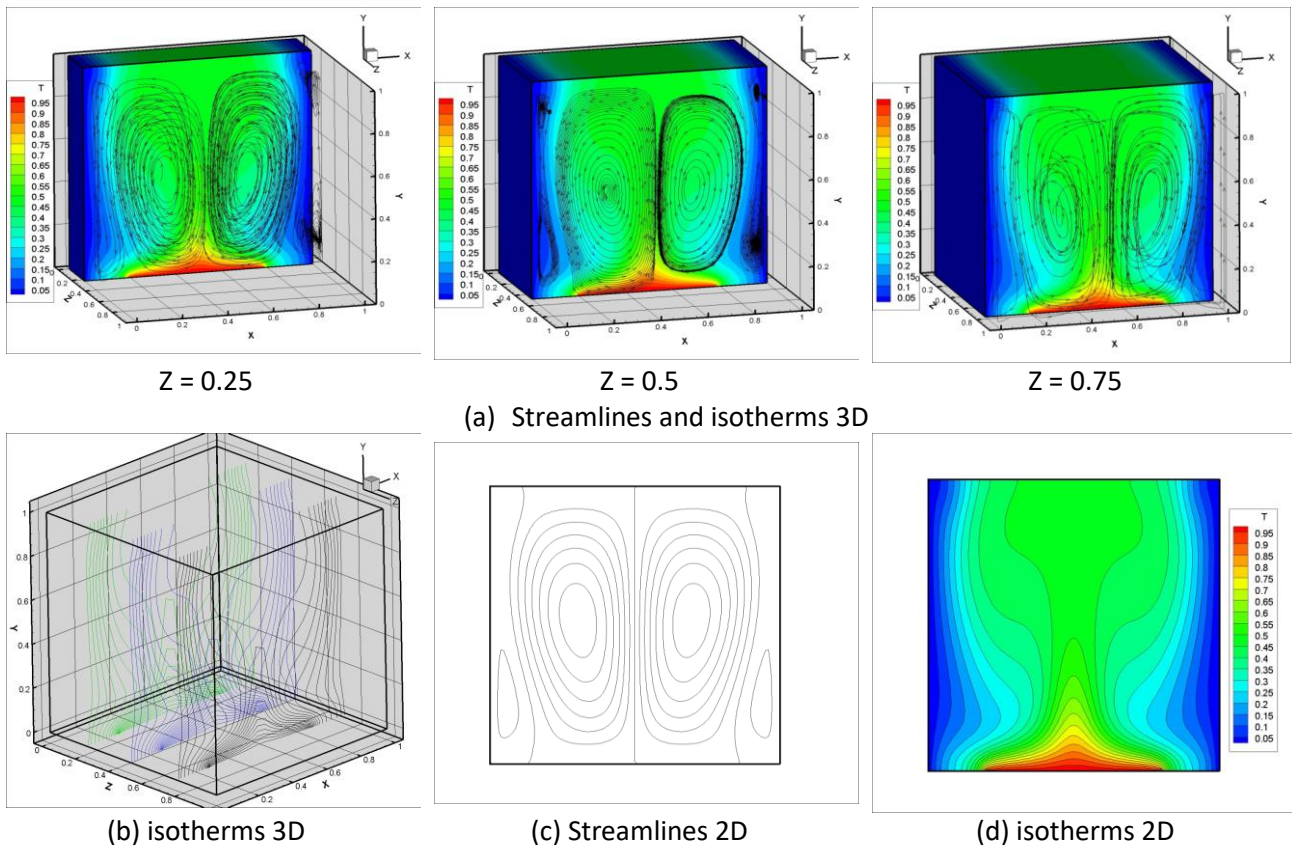


Fig. 5. Streamlines and isotherms for $Re = 100$, Prandtl $Pr = 0.71$ and Richardson number 6.3 , (a,b) 3D case, (c,d) 2D case

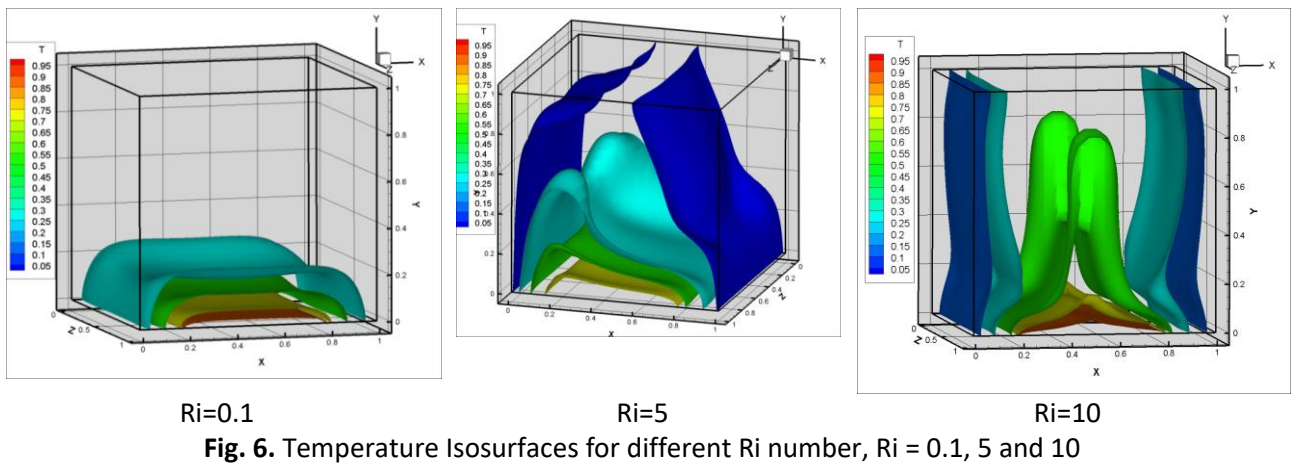


Figure 7 shows the variation of the average Nusselt number as function of Ri number for the 2D and 3D cases, respectively. The overall trend is an increase of Nusselt number with increasing Ri number for both cases and a minor difference could be observed between the two curves. This result confirms that of Hernandez [40]

At low Ri number values ($Ri < 8$), the appearance of minimum and maximum peaks could be obtained which characterize the transition of the heat transfer regimes. The transition from the forced convection (two symmetric vortices) to the mixed convection (two asymmetric vortices) happens at $Ri = 2.51$ and $Ri = 4.7$ for the 3D and 2d cases, respectively. Then, the second transition from mixed convection to natural convection (four symmetrical vortices) happens at $Ri = 6.29$ and $Ri = 7$ for the 3D and 2d cases, respectively.

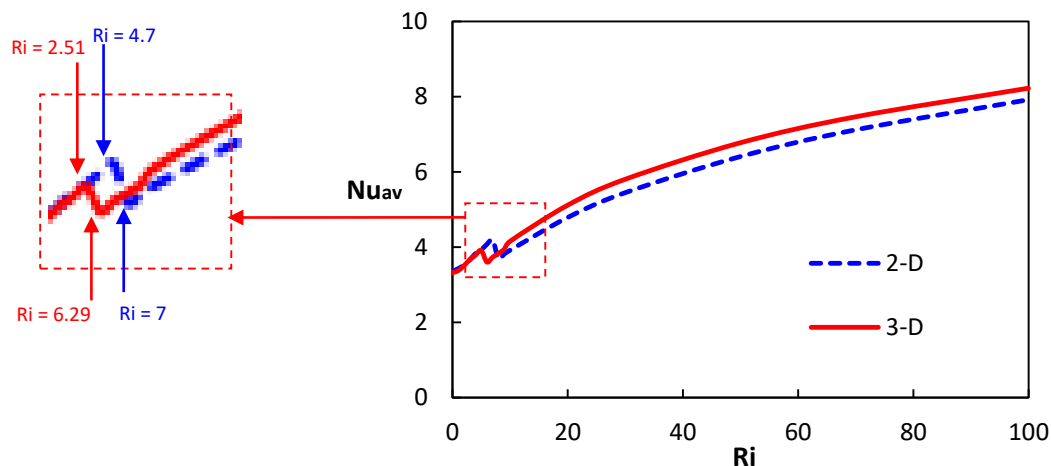


Fig. 7. Average Nusselt number versus Ri number for 2-D and 3-D

6. Conclusions

Numerical investigation for two-dimensional cavity with sliding sidewalls and heated partially from the bottom wall has been performed. Based on the results found in the present study, the following remarks are given.

- I. The flow behaviour was characterized by multiples solutions branches. The heat transfer process was strongly affected by the dominant heat convection regime.
- II. The rate of heat transfer increased in the case of asymmetric branch which is characterized by a dominance of natural convection mode.
- III. The circulations induced by the shear forces prevent the increase of the heat transfer.
- IV. The critical Ri numbers that characterize the transition from the forced convection (two symmetric vortices) to the mixed convection (two asymmetric vortices) and then to the natural convection (four symmetrical vortices) were identified for the 2D and 3d cases, respectively.

References

- [1] Bénard, Henri. "Les tourbillons cellulaires dans une nappe liquide." *Rev. Gen. Sci. Pures Appl.* 11 (1900): 1261-1271.
- [2] Bénard, Henri. "Les tourbillons cellulaires dans une nappe liquide transportant de la chaleur par convection en régime permanent." *Ann. Chim. Phys.* 23, (1901): 62-144.
- [3] Rayleigh, Lord. "LIX. On convection currents in a horizontal layer of fluid, when the higher temperature is on the under side." *The London, Edinburgh, and Dublin Philosophical Magazine and Journal of Science* 32, no. 192 (1916): 529-546.
- [4] Gelfgat, A. Yu, P. Z. Bar-Yoseph, and A. L. Yarin. "Stability of multiple steady states of convection in laterally heated cavities." *Journal of Fluid Mechanics* 388 (1999): 315-334.
- [5] Erenburg, V., A. Yu Gelfgat, E. Kit, P. Z. Bar-Yoseph, and A. Solan. "Multiple states, stability and bifurcations of natural convection in a rectangular cavity with partially heated vertical walls." *Journal of Fluid Mechanics* 492 (2003): 63-89.
- [6] Lappa, Marcello. "On the existence and multiplicity of one-dimensional solid particle attractors in time-dependent Rayleigh-Bénard convection." *Chaos: An Interdisciplinary Journal of Nonlinear Science* 23, no. 1 (2013): 013105.
- [7] Lappa, Marcello. "A mathematical and numerical framework for the simulation of oscillatory buoyancy and Marangoni convection in rectangular cavities with variable cross section." In *Computational Modelling of Bifurcations and Instabilities in Fluid Dynamics*, pp. 419-458. Springer, Cham, 2019.
- [8] Gelfgat, A. (2019) *Computational Modeling of Bifurcations and Instabilities in Fluid Dynamics*, Computational Methods in Applied Sciences. 1st edition. Cham, Switzerland

- [9] Esfe, Mohammad Hemmat, Seyed Sadegh Mirtalebi Esforjani, Mohammad Akbari, and Arash Karimipour. "Mixed-convection flow in a lid-driven square cavity filled with a nanofluid with variable properties: effect of the nanoparticle diameter and of the position of a hot obstacle." *Heat Transfer Research* 45, no. 6 (2014).
- [10] Sivasankaran, S., Ananthan, S. S., Bhuvanewari, M., and Abdulhakeem, A. K. "Double-diffusive mixed convection in a lid-driven cavity with nonuniform heating on sidewalls." *Sādhanā* 42, no. 11 (2017): 1929–1941.
- [11] Kareem, Ali Khaleel, H. A. Mohammed, Ahmed Kadhim Hussein, and Shian Gao. "Numerical investigation of mixed convection heat transfer of nanofluids in a lid-driven trapezoidal cavity." *International Communications in Heat and Mass Transfer* 77 (2016): 195-205.
- [12] El moustaine, B., Cheddadi, A., "Flows Generated by Critical Opposing Thermosolutal Convection in Fluid Annular Cavities." *Journal of Advanced Research in Fluid Mechanics and Thermal Sciences* 50, no.1 (2018): 81-88.
- [13] Yang, K.T. "Transitions and Bifurcations in Laminar Buoyant Flows in Confined Enclosures." *Journal of Heat Transfer, Transactions of the ASME* 110, (1988): 1191-1204.
- [14] Bodenschatz, Eberhard, Werner Pesch, and Guenter Ahlers. "Recent developments in Rayleigh-Bénard convection." *Annual review of fluid mechanics* 32, no. 1 (2000): 709-778.
- [15] Lappa, Marcello. *Thermal convection: patterns, evolution and stability*. John Wiley & Sons, 2009.
- [16] Bairi, Abderrahmane, Esther Zarco-Pernia, and J-M. García De María. "A review on natural convection in enclosures for engineering applications. The particular case of the parallelogrammic diode cavity." *Applied Thermal Engineering* 63, no. 1 (2014): 304-322.
- [17] Hussein, Ahmed Kadhim, Mohamed M. AWAD, Lioua Kolsi, Farshid Fathinia, and I. Adegun. "A comprehensive review of transient natural convection flow in enclosures." *J. Basic Appl. Sci. Res* 4, no. 11 (2014): 17-27.
- [18] Öztop, Hakan F., Patrice Estellé, Wei-Mon Yan, Khaled Al-Salem, Jamel Orfi, and Omid Mahian. "A brief review of natural convection in enclosures under localized heating with and without nanofluids." *International Communications in Heat and Mass Transfer* 60 (2015): 37-44.
- [19] Akhil Soman, P. Anu Nair, Remil Babu, P. K. Sambath Kiran, V. S. Sumesh. "Study on Natural Convection Heat Transfer in an Enclosure—A Review." *IOSR Journal of Mechanical and Civil Engineering (IOSR-JMCE)* 13, no. 4 (2016): 26-30.
- [20] Arun, S., Satheesh, A. Mohan, C.G. Padmanathan, P. Santhoshkumar. D. "A review on natural convection heat transfer problems by Lattice Boltzmann Method." *Journal of Chemical and Pharmaceutical Sciences (JCPS)* 10, no. 1 (2017): 635-645.
- [21] Mohamad, A. A., and R. Viskanta. "Flow structures and heat transfer in a lid-driven cavity filled with liquid gallium and heated from below." *Experimental Thermal and Fluid Science* 9, no. 3 (1994): 309-319.
- [22] Prasad, Ajay K., and Jeffrey R. Koseff. "Combined forced and natural convection heat transfer in a deep lid-driven cavity flow." *International Journal of Heat and Fluid Flow* 17, no. 5 (1996): 460-467.
- [23] Teamah, M. A., MM Abo Elazm, and Ahmed Zaki. "Numerical study of mixed convection heat transfer and fluid flow in cubical lid-driven cavity." *Eur. J. Sci. Res* 72, no. 3 (2012): 460-473.
- [24] Elazm, MM Abo, A. I. Shahata, A. F. Elsafty, and M. A. Teamah. "Numerical Investigation of a Three-Dimensional Laminar Mixed Convection Flows in Lid-Driven Cavity for Very Small Richardson Numbers." In *ASME 2015 Power Conference collocated with the ASME 2015 9th International Conference on Energy Sustainability, the ASME 2015 13th International Conference on Fuel Cell Science, Engineering and Technology, and the ASME 2015 Nuclear Forum*, pp. V001T12A007-V001T12A007. American Society of Mechanical Engineers, 2015.
- [25] Benmansour, Nabil, Nabil Bencheikh, Brahim Ben Beya, and Lili Tong. "Etude numérique de la convection mixte dans une cavité cubique entraînée chauffé par le bas." In *22e Congrès Français de Mécanique*. 2015.
- [26] Sidik, Nor Azwadi Che. "Prediction of natural convection in a square cavity with partially heated from below and symmetrical cooling from sides by the finite difference Lattice Boltzmann Method." *European Journal of Scientific Research* 35, no. 3 (2009): 347-354.
- [27] Benderradji, R., Goudmi, H., Taloub, D. and Beghidja, A., "Numerical study three-dimensional of mixed convection in a cavity: Influence of Reynolds and Grashof numbers." *Journal of Advanced Research in Fluid Mechanics and Thermal Sciences* 51, no.1 (2018): 42-52.
- [28] Mohamad, A. A., and R. Viskanta. "Flow and heat transfer in a lid-driven cavity filled with a stably stratified fluid." *Applied mathematical modelling* 19, no. 8 (1995): 465-472.
- [29] Iwatsu, Reima, and Jae Min Hyun. "Three-dimensional driven-cavity flows with a vertical temperature gradient." *International Journal of Heat and Mass Transfer* 38, no. 18 (1995): 3319-3328.
- [30] Ouertatani, Nasreddine, Nader Ben Cheikh, Brahim Ben Beya, Taieb Lili, and Antonio Campo. "Mixed convection in a double lid-driven cubic cavity." *International Journal of Thermal Sciences* 48, no. 7 (2009): 1265-1272.
- [31] Benkacem, N., Ben Cheikh, N. and Ben Beya, B. "Three-dimensional Analysis of Mixed Convection in a Differentially Heated Lid-driven Cubic Enclosure." *J. Appl. Mech. Eng.* 4 (2015): 159.

- [32] Rani, H.P., Narayana V. and Rameshwar, Y. "Analysis of vortical structures in a differentially heated lid driven cubical cavity." *Int. J. Heat and Technology* 36, no. 2 (2018): 548-556.
- [33] Nor Azwadi, C. S., and T. Tanahashi. "Three-dimensional thermal lattice Boltzmann simulation of natural convection in a cubic cavity." *International Journal of Modern Physics B* 21, no. 01 (2007): 87-96.
- [34] Guo, Guanghong, and Muhammad AR Sharif. "Mixed convection in rectangular cavities at various aspect ratios with moving isothermal sidewalls and constant flux heat source on the bottom wall." *International journal of thermal sciences* 43, no. 5 (2004): 465-475.
- [35] Yang, Orhan Aydin, Wen-Jei. "Mixed convection in cavities with a locally heated lower wall and moving sidewalls." *Numerical Heat Transfer: Part A: Applications* 37, no. 7 (2000): 695-710.
- [36] Khaleel Kareem, A. and Gao, S. "CFD Investigation of Turbulent Mixed Convection Heat Transfer in a Closed Lid-Driven Cavity." *International Journal of Civil, Environmental, Structural, Construction and Architectural Engineering* 9, no. 12 (2015): 1546-1551.
- [37] Khaleel Kareem, A., Gao Shian and Ahmed Qasim Ahmed. "Unsteady simulations of mixed convection heat transfer in a 3D closed lid-driven cavity." *International Journal of Heat and Mass Transfer* 100, (2016): 121-130.
- [38] Kareem, Ali Khaleel, and Shian Gao. "Computational study of unsteady mixed convection heat transfer of nanofluids in a 3D closed lid-driven cavity." *International Communications in Heat and Mass Transfer* 82 (2017): 125-138.
- [39] Patankar, Suhas (1980). *Numerical Heat Transfer and Fluid Flow*, McGraw-Hill, New York.
- [40] Hernandez, R. H. "Natural convection in thermal plumes emerging from a single heat source." *International Journal of Thermal Sciences* 98 (2015): 81-89.